Intrinsic Structural and Functional Determinants within the Amino Acid Sequence of Mature Pulmonary Surfactant Protein SP-B†

Alicia G. Serrano,‡ Antonio Cruz,‡ Karina Rodríguez-Capote,§ Fred Possmayer,§ and Jesús Pérez-Gil*,‡

Departamento de Bioquímica, Facultad de Biología, Universidad Complutense, Madrid, Spain, and Departments of Obstetrics and Gynecology and of Biochemistry, University of Western Ontario, London, Canada

Received June 11, 2004; Revised Manuscript Received October 13, 2004

ABSTRACT: Pulmonary surfactant protein SP-B is absolutely required for proper function of surfactant in the alveoli, and is an important component of therapeutical surfactant preparations used to treat respiratory pathologies. To explore inherent structural and functional determinants within the amino acid sequence of mature SP-B, porcine SP-B has been subjected to extensive disulfide reduction under highly denaturing conditions and to cysteine carboxyamidomethylation, and the structure, lipid−protein interactions, and surface activity of this modified form have been characterized. Refolding of the reduced protein yielded a form (SP-Br) with secondary structure practically identical to that of the native disulfide-linked SP-B dimer. Reduced SP-Br exhibited higher structural flexibility than native SP-B, as indicated by a higher susceptibility of fluorescence emission to quenching by acrylamide and biphasic behavior during interaction of the protein with lipid bilayers and monolayers. SP-Br had, however, effects similar to those of native SP-B on the thermotropic properties of dipalmitoylphosphatidylcholine (DPPC) bilayers. SP-Br was more effective than native SP-B in promoting interfacial adsorption of phospholipid bilayers into interfacial films, presumably because of its higher structural flexibility, and retained the ability of native SP-B to stabilize DPPC interfacial films compressed to pressures near collapse against spontaneous relaxation. SP-Br also mimicked the behavior of native SP-B in lipid−protein films subjected to dynamic compression−expansion cycling in a captive bubble surfactometer, but only in the presence of phosphatidylglycerol (PG), the main anionic phospholipid in surfactant. The presence of PG appears to be required for SP-Br to acquire the appropriate tertiary folding to produce progressively more efficient lipid−protein films capable of reaching very high pressures upon limited compression with almost no hysteresis.

Pulmonary surfactant protein SP-B is an essential polypeptide required for maintaining patent gas-exchange surfaces in mammalian lungs (*1*). SP-B functions as part of pulmonary surfactant, a lipid−protein complex synthesized and secreted by the alveolar epithelium of lungs. The major role of surfactant is to reduce surface tension at the air−liquid interface, thereby facilitating alveolar expansion during inspiration and preventing their collapse at the end of expiration. Pulmonary surfactant contains ∼90% lipids, mainly phospholipids, with the main surface active component being dipalmitoylphosphatidylcholine (DPPC)[1] (*2*). SP-B contributes toward the transference of phospholipid molecules from bilayers in lamellar bodies, the structural form in which surfactant is assembled by the pneumocytes, to surface-active interfacial films (*3*, *4*). Genetic inactivation of the SP-B gene, either *in utero* (*5*, *6*) or in the adult (*7*), induces irreversible and lethal respiratory failure, because of the inability to maintain adequate respiratory function. Premature babies with immature lungs that lack sufficient pulmonary surfactant often suffer from neonatal respiratory distress syndrome (NRDS), but this pathology can now be treated and even prevented by supplementation with exogenous surfactant preparations (*8*). Other pathologies originating as acute lung injury (ALI) in either infants or adults inactivate the surfactant system as a secondary consequence, resulting in the development of acute respiratory distress syndrome (ARDS). The use of exogenous surfactant to treat these latter pathologies is under investigation. Such therapies will depend on the production of sufficient amounts of highly active surfactant preparations with high resistance to inhibition (*9*). Most therapeutic surfactant preparations currently

† Research in the laboratory of some of the authors (A.G.S., A.C., and J.P.-G.) has been funded by grants from DGESIC (BIO2003-09056) and CAM (08.2/0054.1/2001), Spain, and work by F.P. has been supported by a Group Grant from the Canadian Institutes of Health Research. K.R.-C. acknowledges a CIHR/Canadian Lung Foundation Fellowship.

* To whom correspondence should be addressed: Departamento de Bioquímica, Facultad de Biología, Universidad Complutense, 28040 Madrid, Spain. Phone: +34 91 3944994. Fax: +34 91 3944672. E-mail: jpg@bbm1.ucm.es.

‡ Universidad Complutense.

§ University of Western Ontario.

[1] Abbreviations: ALI, acute lung injury; ARDS, acute respiratory distress syndrome; CBT, captive bubble tensiometer; CCA, convex constraint analysis; Chl, chloroform; DPPC, 1,2-dipalmitoylphosphatidylcholine; DPPG, 1,2-dipalmitoylphosphatidylglycerol; DTT, dithiothreitol; GndCl, guanidinium chloride; IAA, iodoacetamide; LPC, 1-palmitoyl-2-lysophosphatidylcholine; MALDI-TOF, matrix-assisted laser desorption ionization time-of-flight; MeOH, methanol; NRDS, neonatal respiratory distress syndrome; POPC, 1-palmitoyl-2-oleoylphosphatidylcholine; POPG, 1-palmitoyl-2-oleoylphosphatidylglycerol; PC, 1,2-diacylphosphatidylcholine from egg yolk; PG, 1,2-diacylphosphatidylglycerol from egg yolk; SP-B, surfactant protein B; SP-Br, reduced and alkylated surfactant protein B; SUV, small unilamellar vesicles; TFE, trifluoroethanol.

10.1021/bi048781u CCC: $30.25
Published on Web 12/10/2004

used in respiratory medicine are obtained from animal sources and contain SP-B as an important constituent. Native SP-B as purified from lung surfactant consists of a disulfide-linked homodimer of two 79-residue polypeptides. SP-B is very hydrophobic in nature, and its three-dimensional structure has not been determined (*10*). Various studies have concluded that the structure of SP-B is dominated by several cationic amphipathic α-helices. These presumably interact with the surface of surfactant bilayers or monolayers (*3*). Production of human versions of SP-B by recombinant technology has been hampered by the fact that the native mature protein contains seven cysteines among its 79 residues, which form three intramolecular disulfide bonds and one intermolecular disulfide bond (*11*). *In vivo*, SP-B is produced in type II pneumocytes through maturation of a much larger precursor, by a tissue-specific processing pathway (*12*). On the other hand, synthetic peptides with sequence corresponding to part of the putative amphipathic helical regions of SP-B appear to mimic many of the lipid−protein interactions and surface activities of the native protein (*13*, *14*). This observation suggests the possibility that polypeptides with the mature sequence of SP-B but lacking disulfides could act as efficient analogues for developing new human-compatible surfactant preparations. In this work, we have studied the structure, lipid−protein interactions, and surface activity of porcine SP-B after extensive reduction and alkylation of its cysteines, and compared these properties with those of the native form. We conclude that the primary SP-B sequence contains inherent tertiary structural and functional determinants, suggesting that it should be possible to generate highly active synthetic SP-B mimics.

EXPERIMENTAL PROCEDURES

Materials. Chloroform (Chl) and methanol (MeOH) were HPLC grade solvents from Scharlau (Barcelona, Spain). Sephadex LH-20 and LH-60 chromatography gels were obtained from Pharmacia (Uppsala, Sweden). Phospholipids 1,2-dipalmitoyl-*sn*-glycero-3-phosphocholine (DPPC), egg yolk phosphatidylcholine (PC), 1,2-dipalmitoyl-*sn*-glycero-3-[phospho-*rac*-(1-glycerol)] (DPPG), 1-palmitoyl-2-oleoylphosphatidylcholine (POPC), 1-palmitoyl-2-oleoylphosphatidylglycerol (POPG), and 1-palmitoyl-2-lysophosphatidylcholine (LPC) were from Avanti Polar Lipids (Birmingham, AL). Egg yolk phosphatidylglycerol (PG), dithiothreitol (DTT), and iodoacetamide (IAA) were obtained from Sigma (St. Louis, MO). Trifluoroethanol (TFE) and all other reagents and chemicals were purchased from Merck (Darmstadt, Germany).

SP-B Purification. Surfactant protein SP-B was isolated from minced porcine lungs by an adaptation of the method of Curstedt et al. (*15*), which is described elsewhere (*16*). After isolation, solutions of purified SP-B in a 2:1 (v/v) Chl/MeOH mixture were stored at −20 °C until they were used. The purity of the protein was routinely checked by SDS−PAGE and quantitated by amino acid analysis on a Beckman model 6300 automatic analyzer equipped with an IBM-AT-based System Gold enhancement.

SP-B Reduction and Alkylation. Reduction of the disulfide bonds of SP-B and subsequent carboxyamidomethylation of the resulting thiol groups were performed as follows. SP-B (protein concentration of 20 μg/mL) was kept overnight at room temperature in a methanolic solution (apparent pH 8.0) containing 4 M guanidinium chloride (GndCl). Reduction of the disulfide bridges was achieved by addition of DTT to a final concentration of 50 mM and incubation at 37 °C for 2 h. IAA was then added to a final concentration of 500 mM, and the mixture was incubated in the dark for 90 min at 37 °C. The reduced and alkylated SP-B (SP-Br) was freed of unreacted reagents by extensive dialysis and subsequent LH-20 chromatography with a 2:1 (v/v) Chl/MeOH mixture. The state of oligomerization of SP-B after reduction and carboxyamidomethylation was analyzed by SDS electrophoresis using 16% acrylamide gels in a Mini-Protean II (Bio-Rad) chamber. Protein bands were detected by silver staining.

Mass Spectrometry. Protein bands of interest were excised from the Coomassie Blue-stained gels, and in-gel tryptic digestion was performed using an adaptation of the method of Schevchenko et al. (*17*), in a digestor Investigator ProGest (Genomic Solutions, Cambridgeshire, United Kingdom) (*18*). Briefly, the gel slices were washed with 25 mM NH_4HCO_3 and CH_3CN several times, and then dried under a N_2 stream. Gel pieces were then incubated for 12 h at 37 °C with 16 ng/μL (final concentration) porcine trypsin (Promega, Madison, WI) in 25 mM NH_4HCO_3. Peptides were eluted with CH_3CN, 25 mM NH_4HCO_3, and 10% (v/v) HCOOH in a final volume of 100 μL. Samples were then automatically analyzed by matrix-assisted laser desorption ionization mass spectrometry in a Bruker Reflex III MALDI-TOF mass spectrometer (Bruker-Franzen Analytic GmbH, Bremen, Germany), in the positive ion reflection mode with delayed ion extraction (*19*). The accelerating voltage was 25 kV. External calibration was performed with a mixture of peptides in the *m*/*z* range of 1000−4000, and all spectra were internally calibrated using autodigestion peptides from porcine trypsin such that the unknown peptide masses were accurate to within 30 ppm.

Reconstitution of Protein/Phospholipid Samples. To reconstitute SP-B or SP-Br in phospholipid bilayers or micelles of lysophosphatidylcholine, the lipids (DPPC, DPPG, PC, PG, and LPC) were first mixed with the appropriate amounts of protein in a 2:1 (v/v) Chl/MeOH mixture. The mixture was dried under a N_2 stream and then under vacuum overnight. The resulting dried films were hydrated by addition of 1 mL of 5 mM Tris buffer (pH 7) containing 150 mM NaCl and incubated for 1 h with intermittent vortexing, at room temperature for PC and PG (or LPC) and at 50 °C for DPPC and DPPG. This treatment typically produces suspensions of multilamellar phospholipid vesicles. To obtain small unilamellar vesicles (SUV) or lysophospholipid micelles, the lipid or lipid/protein suspensions were sonicated (on ice for PC, PG, and LPC or at room temperature for DPPC and DPPG) in a Branson UP200S tip sonifier at 360 W/cm^2 for two 1 min cycles.

Circular Dichroism. Far-UV circular dichroism (CD) spectra of protein or lipid/protein samples were recorded as described previously (*20*) in a Jasco 715 spectropolarimeter equipped with a xenon lamp. Aliquots of 100 μg of protein were reconstituted in phospholipid SUV at a final protein:lipid ratio of 1:5 (w/w), in 1 mL of 5 mM Tris buffer (pH 7) containing 150 mM NaCl. The final protein concentration of each sample was re-evaluated by amino acid analysis. All the spectra were recorded in a 0.2 mL thermostated quartz

cell with an optical path length of 0.1 cm. Ellipticity was calculated taking 110 as the mean molecular weight per residue in SP-B. Estimation of the secondary structure content from the CD spectra was performed after deconvolution of the spectra into four simple components (α-helix, β-sheet, turns, and random coil) according to the convex constraint algorithm (CCA) (*21*).

Intrinsic Fluorescence of SP-B and SP-Br. Tryptophan fluorescence emission spectra of SP-B or SP-Br in organic solvents or lipid environments were recorded either in a Perkin-Elmer MPF-44E or in a SLM-Aminco AB-2 spectrofluorimeter operated in the ratio mode using 275 nm as the excitation wavelength (*22*). Spectra were obtained at 25 °C from samples in organic solvents or in PC suspensions, and at 45 °C for DPPC/protein samples, in thermostated cells with an optical path length of 0.2 cm. The slit widths were 7 and 5 nm for the excitation and emission beams, respectively, and the scanning speed was 1 nm/s.

The parameters governing the association of SP-B or SP-Br with PC or DPPC bilayers were determined from the changes in the fluorescence emission spectrum of the proteins upon their reconstitution with variable amounts of phospholipid. In these experiments, samples were first prepared by mixing the appropriate amounts of protein and lipid in a small volume (20 μL) of a methanolic solution. Lipid and lipid/protein bilayers were then formed by injecting this methanolic solution into 0.5 mL of 50 mM HEPES buffer (pH 7) containing 150 mM NaCl, under vigorous vortex mixing, at room temperature for PC samples or 50 °C for DPPC-containing suspensions. This method has been demonstrated to produce homogeneous uni- or paucilamellar vesicles ∼100−200 nm in diameter (*23*). Controls were prepared by injecting identical volumes of methanol in the absence of protein and/or lipid.

Fluorescence spectra were corrected for the scatter contribution due to lipid dispersions by subtracting the corresponding control spectra obtained in the absence of protein. In addition, an inner-filter correction was applied to the emission spectra according to the equation

$$F_c = F_m \times 10^{(A_{em}+A_{ex})/2}$$

where F_c is the corrected fluorescence intensity, F_m is the measured fluorescence intensity after correction for scattering, and A_{em} and A_{ex} are the absorbances measured at the emission and excitation wavelengths, respectively (*24*). Absorption spectra of the samples were recorded using a Beckman DU-640 spectrophotometer.

Fluorescence Quenching Experiments. Aliquots (1−2 μL) of 2.5 mM acrylamide in methanol were added to SP-B or SP-Br methanolic solutions, and the fluorescence emission spectra were recorded from 300 to 440 nm after each addition. Data were corrected for dilution and analyzed by the classical Stern−Volmer equation for collisional quenching (*25*), to calculate the Stern−Volmer dynamic quenching constant, K_{sv}.

Differential Scanning Calorimetry. Dried samples of 1 mg of DPPC in the absence or presence of 5 or 10% protein were dispersed in 1 mL of 50 mM HEPES buffer (pH 7) containing 150 mM NaCl to form multilamellar suspensions. An aliquot of 0.47 mL of this suspension was loaded in the sample cell of either a DASM-4 or VP-DSC microcalorimeter (Microcal, Northhampton, MA) (*26*), with buffer in the reference cell. Five calorimetric scans were collected from each sample between 25 and 70 °C at a rate of 0.5 °C/min.

Interfacial Adsorption. Interfacial adsorption of lipid and lipid/protein samples was assayed using a specially designed surface balance similar to that described previously (*23*, *27*, *28*). This balance contained 1.5 mL of subphase at 25 °C, and the change in surface pressure (π) during adsorption from vesicles was monitored with a Wilhelmy dipping plate of Whatman No. 1 paper attached to the pressure transducer. Two hundred micrograms of DPPC containing 0, 5, or 10% protein (w/w), reconstituted in 200 μL of 5 mM Tris buffer (pH 7) containing 150 mM NaCl and 5 mM $CaCl_2$, was injected into 1.5 mL of the subphase of the same buffer while being continuously stirred. Interfacial adsorption was monitored by measuring the changes in surface pressure with time.

Compression Isotherms. Monolayers of pure protein, pure lipid, or lipid/protein binary systems were formed by spreading 20−30 μL of the concentrated solutions in a 3:1 (v/v) Chl/MeOH mixture at the surface of a 5 mM Tris-HCl subphase (pH 7) containing 150 mM NaCl in a thermostated Langmuir−Blodgett trough (NIMA Technologies, Coventry, United Kingdom) which employed a continuous Teflon ribbon barrier to minimize film leakage at high surface pressures. Subphases were prepared with doubly distilled water, and the second distillation was performed from dilute potassium permanganate. After each monolayer had been spread, the organic solvent was allowed to evaporate for 10 min before compression was started. The total area of the interface at the beginning of each experiment was 174 cm^2, and the monolayer was compressed at 65 cm^2/min while the changes in surface pressure were monitored with a Wilhelmy dipping plate attached to the force transducer.

To analyze the effect of SP-B and SP-Br on the stability of compressed phospholipid monolayers, lipid or lipid/protein films were compressed up to 70 mN/m before the spontaneous surface pressure decay versus time was monitored, as previously described (*28*).

Captive Bubble Surfactometry. Adsorption isotherms were also recorded from multilamellar suspensions of DPPC/POPC (70:30, w/w) and DPPC/POPG (70:30, w/w) lipid mixtures with or without 1 wt % protein (SP-B or SP-Br) in a custom-designed captive bubble tensiometer (CBT) (*29*). After the CBT chamber was filled with the appropriate lipid/protein sample reconstituted in 2 mM Tris-HCl buffer (pH 7), 150 mM NaCl, and 1.5 mM $CaCl_2$ and the temperature was equilibrated at 37 °C, an air bubble ∼8 mm in diameter was introduced into the suspension. The change in bubble shape was recorded to monitor the adsorption of material to the bubble air−water interface. After adsorption was complete, the bubble chamber was sealed, and quasi-static or dynamic compression−expansion of the bubble was performed as described elsewhere (*29*). Images documenting changes in bubble area were recorded during each individual experiment, and bubble shapes were analyzed using custom-designed software (*30*).

Statistics. Unless otherwise indicated, most results have been presented as representative experiments after repeated examination of three different samples from at least two different batches of native SP-B or reduced SP-Br. Results from captive bubble surfactometry have been plotted as

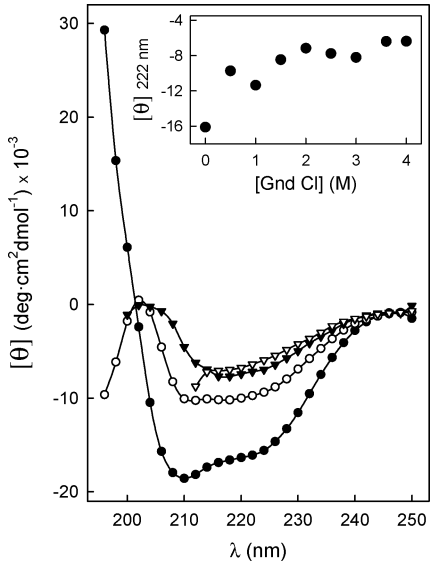

FIGURE 1: Circular dichroism spectra of SP-B in the presence of guanidinium chloride. Far-UV circular dichroism spectra of native SP-B in methanol, in the absence (●) or presence of 0.5 (○), 2 (▼), or 4 M GndCl (▽). The inset shows the molar ellipticity at 222 nm of SP-B in methanol vs the concentration of GndCl. Samples were prepared by O/N incubation at room temperature of 90 μg/mL native SP-B in methanol, in the presence of the indicated concentrations of GndCl.

means with error bars indicating the standard deviation after three to five different experiments had been averaged.

RESULTS

Treatment of purified SP-B with DTT followed by thiol blockage with iodoacetamide resulted in the appearance of monomeric forms that are not present in the native protein preparations, which are only dimeric as purified from the lungs (see, for instance, ref *16*). When we tried this procedure in the past, we always detected a significant proportion of the protein that remained dimeric after treatment. To produce extensive reduction of SP-B, we have optimized a reductive procedure under denaturing conditions, as detailed in Experimental Procedures. Figure 1 shows that preincubation of SP-B in methanol with concentrations of the chaotropic agent guanidinium chloride (GndCl) higher than 2 M yields a highly denatured form of the protein, as judged from its CD spectrum. Estimations from the CD spectra using the CCA method indicate that SP-B contains around 50% α-helical conformation in methanol but retains only marginal proportions of α-helix in the presence of >2 M GndCl. Figure 2a shows that native SP-B can be converted, after extensive reduction and alkylation in the presence of 4 M GndCl, into a preparation containing mainly monomeric forms. Production of SP-B monomers is maximal when the protein is reduced at low concentrations. Treatment of SP-B at protein concentrations higher than 30 μg/mL produces a mixture of monomers and *n*-mers in different proportions. To determine whether the reduction reaction cleaved also the intramolecular disulfides in SP-B, we analyzed the mass of the peptides liberated upon proteolytic treatment of both native (SP-B) and reduced (SP-Br) proteins. Figure 2b shows MALDI-TOF mass spectrograms of samples of SP-B and SP-Br in the molecular mass:charge ratio range of 800−2000. Peaks with the indicated masses in the spectrograms have been assigned according to the scheme drawn in Figure 2c, where the amino acid sequence, the position of the disulfides, and the molecular mass of tryptic peptides expected from the porcine protein have been summarized. The tryptic digestion patterns of SP-B and SP-Br differed substantially. Incubation of native SP-B with trypsin produced mainly minor peaks in the scanned mass range, with a major peak with a mass of 910.5. Figure 2c allows identification of this peak as one of the only two peptides

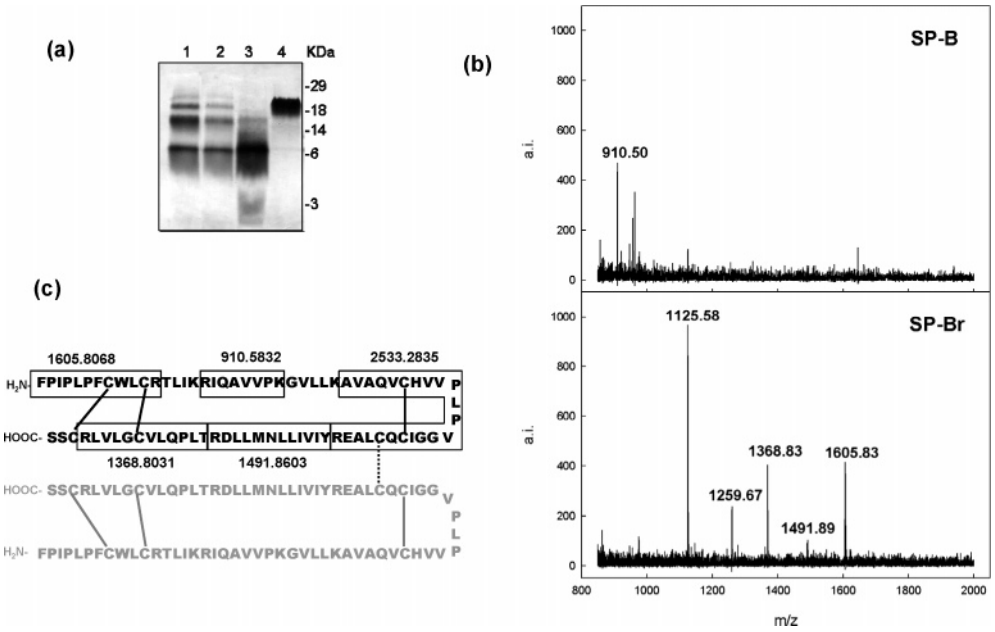

FIGURE 2: Analysis of reduced and alkylated SP-B (SP-Br). (a) Effect of protein concentration on the oligomeric state of SP-B after reduction and subsequent carboxyamidomethylation. Lanes 1−3 contained 8 μg of protein treated at 2000, 80, and 8 μg/mL, respectively. Lane 4 contained 8 μg of native SP-B. (b) MALDI-TOF mass spectrometry analysis of native SP-B and SP-Br after digestion with porcine trypsin. The molecular weight/charge ratios corresponding to the major peaks are given. (c) Position of disulfide bonds in the sequence of SP-B. The boxes denote peptides expected from tryptic treatment of SP-Br, including their theoretical molecular mass calculated by considering completely reduced and alkylated cysteines and oxidized methionines.

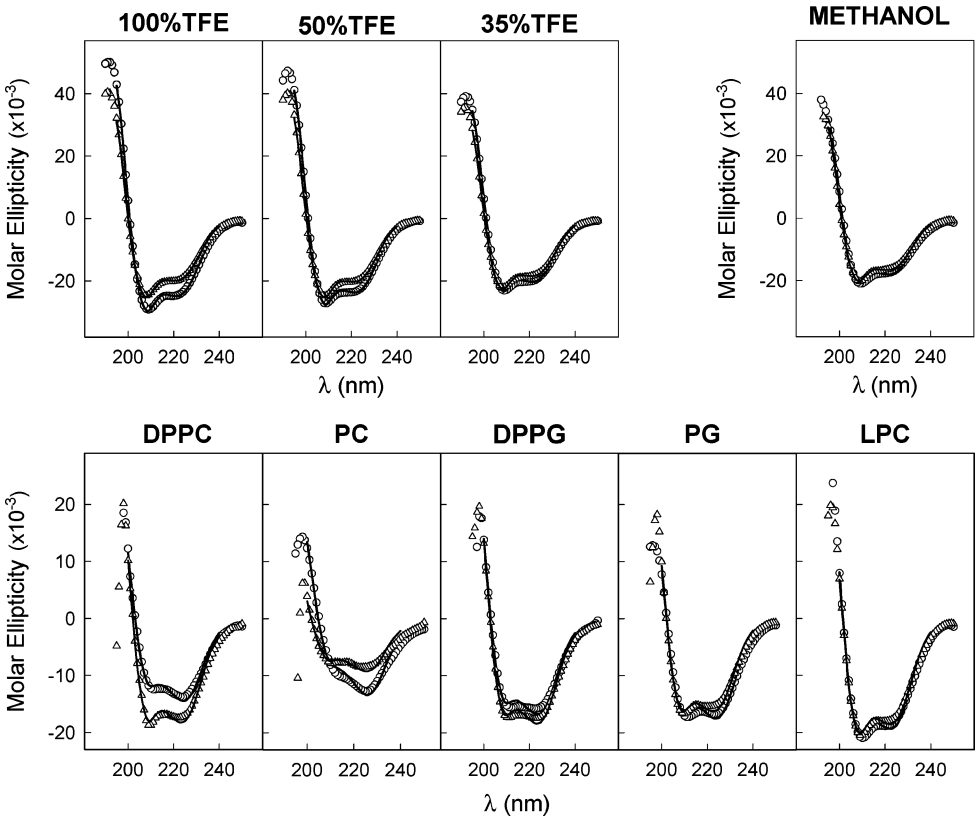

FIGURE 3: Circular dichroism spectra of SP-B and SP-Br in organic solvents and lipids. The top panels show far-UV circular dichroism spectra of native SP-B (○) and SP-Br (△) in aqueous mixtures of TFE containing the indicated proportions of organic solvent (left) and in methanol (right). The bottom panel shows far-UV circular dichroism spectra of native SP-B (○) and SP-Br (△) in SUV of the indicated phospholipids or in LPC micelles. Solid lines represent the theoretical spectra for the secondary structural parameters calculated according to the convex constraint analysis (*21*) and summarized in Table 1.

within this mass range that should be liberated by trypsin digestion of native SP-B, provided all the disulfides are maintained. Digestion by trypsin of SP-Br liberates a different set of peptides (Figure 2b, bottom panel) that were not produced upon trypsinization of native SP-B. Two of these peptides, with masses of 1368.8 and 1605.8, corresponded to fragments that could only be produced by proteolysis of SP-Br if at least two of the three intramolecular disulfide bonds were opened. The spectrogram of SPBr shown in Figure 2b does not contain the peak at *m*/*z* 910, but this peptide could be observed with relatively low intensity in other samples of SP-Br (not shown). That peptide contains an additional tryptic target, which when hydrolyzed liberates a peptide of 754 Da, out of the mass range we have scanned in our spectrograms.

The effect of disulfide reduction on the secondary structure of SP-Br was analyzed by circular dichroism (CD). Figure 3 shows the far-UV CD spectra of native SP-B and SP-Br in organic solutions and in reconstituted lipid suspensions. The spectra of SP-Br were qualitatively comparable, in all the assayed environments, to the spectra of native SP-B. The two protein forms exhibited CD features consistent with a mainly α-helical conformation, including ellipticity minima at 222 and 207 nm and a marked maximum at 195 nm. Table 1 summarizes the relative proportions of the different types of secondary structure calculated from the CD spectra of the two proteins, native SP-B and SP-Br, in the different environments, using the CCA algorithm proposed by Perczel et al. (*21*). Native SP-B contains ∼50% α-helix and 18% *β*-sheet in methanol and aqueous trifluoroethanol (TFE), with the percent of helix increasing up to ∼60% in pure TFE. In lipids, the helical content of SP-B ranges from 40 to 45% in zwitterionic bilayers, increasing to 50−55% in anionic membranes made of PG up to a maximum of 60% when included in micelles of LPC. Similar environment-dependent conformational variations have been described previously (*16*). SP-Br is calculated to possess ∼50% α-helix in all the organic solvents that have been tested, which increases to 55−60% in lipid membranes or micelles.

Table 1: Secondary Structure of Native SP-B and SP-Br in Methanol and TFE/Water Mixtures and Included in Phospholipid Vesicles or LPC Micelles, Estimated from Their Far-UV Circular Dichroism Spectra by the Convex Constraint Analysis

	% secondary structure							
	SP-B				SP-Br			
	α	*β*	*T*	*R*	α	*β*	*T*	*R*
methanol	50	18	9	23	49	11	14	26
100% TFE	61	11	0	28	49	10	2	39
50% TFE	57	19	0	24	49	11	2	38
35% TFE	51	17	5	27	47	0	29	24
DPPC	41	–	–	–	58	–	–	–
PC	43	–	–	–	–	–	–	–
DPPG	56	–	–	–	55	–	–	–
PG	50	–	–	–	54	–	–	–
LPC	59	–	–	–	59	–	–	–

The slight differences detected between the secondary structure of native SP-B and SP-Br are not associated with significant differences in the fluorescence properties of the protein. Figure 4 illustrates that the fluorescence emission spectra of the two proteins, native SP-B and SP-Br, were

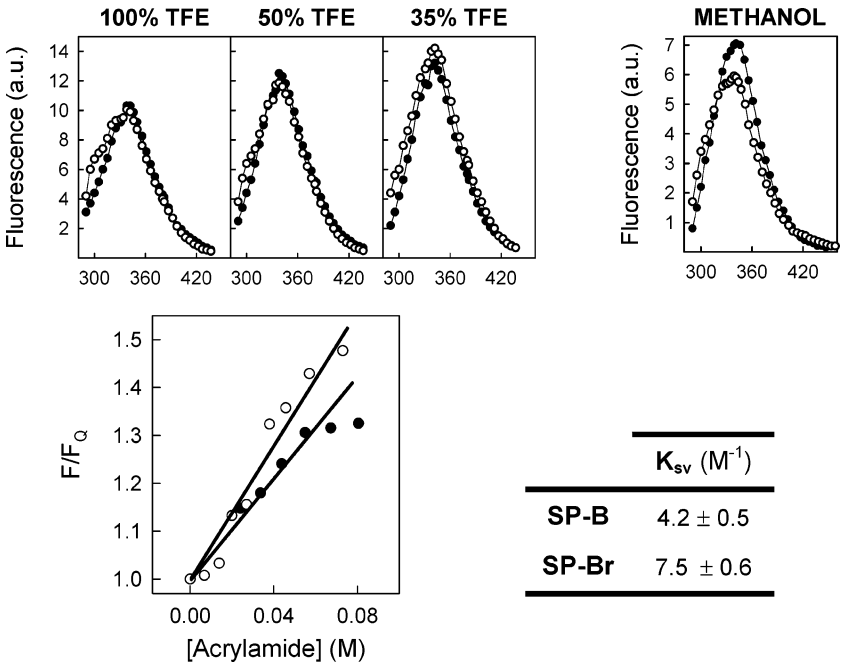

FIGURE 4: Fluorescence emission spectra of SP-B and SP-Br in organic solvents. The top panels show fluorescence emission spectra of native SP-B (●) and SP-Br (○) in aqueous mixtures of TFE containing the indicated proportions of organic solvent (left) and in methanol (right). The excitation wavelength was 275 nm, and the emission intensity is presented in arbitrary units. The bottom panel shows quenching by acrylamide of the fluorescence emission of native SP-B (●) and SP-Br (○) in a methanolic solution. Excitation and emission wavelengths were 295 and 340 nm, respectively. The calculated Stern−Volmer constants for dynamic quenching of fluorescence from both SP-B and SP-Br by acrylamide are summarized in the table.

comparable in aqueous or pure TFE or in methanol. Interestingly, the Stern−Volmer constant for the quenching of tryptophan fluorescence by acrylamide in methanol was almost twice as high for SP-Br as for native SP-B (Figure 4, bottom panels), indicating a somewhat higher accessibility of tryptophan to quencher in SP-Br than in the disulfide-cross-linked native form of SP-B. Figure 5 provides a detailed analysis of the fluorescence emissions of native SP-B and SP-Br in phospholipid membranes, as a function of the lipid:protein ratio. Titration of the effects of the lipid−protein interactions on the fluorescence properties of SP-B has been used previously to estimate the parameters governing interactions of the protein with lipid membranes, including the apparent lipid:protein stoichiometry at saturation, *n*, and the relative affinity constant, K_D (*22*, *31*). Both protein forms, the native SP-B and SP-Br, increase their intrinsic tryptophan fluorescence emission as they are reconstituted with increasing amounts of lipids. The increase in fluorescence intensity of the two proteins approaches a limit at high lipid:protein ratios. The change in fluorescence was then used to estimate the amount of lipid-bound and lipid-free forms of the two proteins at the different lipid:protein ratios, as described elsewhere (*22*). Fitting the resulting binding curve to a classical Scatchard plot is depicted in the insets of Figure 5. Binding of native SP-B to either DPPC or egg yolk PC could be reasonably well fitted to linear Scatchard behavior, as previously reported, yielding estimations of around 20 for the lipid−protein stoichiometry *n* (see Table 2) and K_D values in the micromolar range. However, the Scatchard plots corresponding to the binding data for the reduced form, SP-Br, clearly showed biphasic distributions in both DPPC and egg PC membranes. We have tentatively fitted the two segments of the plots and included the two sets of calculated K_D values in Table 2. Although the actual meaning of these numbers remains undetermined, this analysis seems to indicate that, after reduction, SP-Br binds to lipids in a more complex way that could imply the existence of two distinct binding events. At low lipid:protein ratios, the protein could bind to the lipids with an apparent affinity higher than that of the nonreduced protein, while at high lipid:protein ratios, the changes in the fluorescence of SP-Br are consistent with a much lower protein−lipid binding affinity.

Figure 6 compares the effects of native SP-B and SP-Br on the thermotropic properties of DPPC bilayers. Both protein forms abrogated the pretransition and produced a prominent broadening of the main calorimetric peak associated with the gel-to-liquid crystalline phase transition that occurs at 41 °C with pure DPPC. Table 3 summarizes the parameters determined for the thermotropic transitions of DPPC bilayers in the absence and presence of native SP-B or SP-Br. Both proteins reduced to similar extents the enthalpy associated with the main calorimetric peak. This peak was shifted to higher temperatures in the presence of either of the two proteins. The effect of the two SP-B forms is qualitatively and quantitatively similar to that previously reported for native porcine SP-B (*32*), indicating that the reduced protein interacts with and perturbs the packing of the acyl chains of DPPC in a manner similar to that of the native disulfide-linked protein.

Finally, we have compared the surface properties imparted by either native SP-B or SP-Br to phospholipids. Figure 7 analyzes the effect of disulfide reduction on the ability of SP-B to promote rapid adsorption of phospholipids from bilayers into interfacial surface-active films. Interfacial adsorption of SP-B-containing bilayers has been studied using both a classical King−Clements device allowing direct monitoring of the increase in surface pressure associated with interfacial adsorption at 25 °C and a CBT allowing evaluation

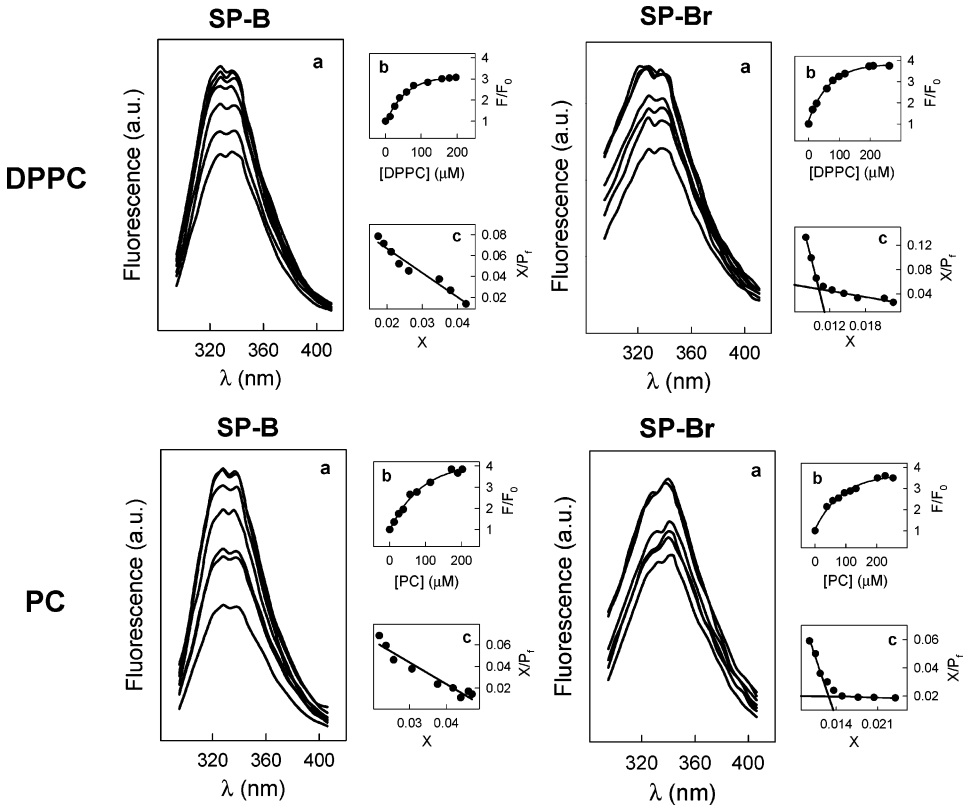

FIGURE 5: Effect of lipid−protein interactions on the fluorescence properties of SP-B and SP-Br in phospholipid bilayers. (a) Fluorescence emission spectra of SP-B (4 μM) or SP-Br (1.5 μM) injected into 50 mM HEPES buffer (pH 7) containing 150 mM NaCl, in the absence or presence of increasing amounts (from the bottom to the top spectra) of DPPC (top panels) or egg yolk PC (bottom panels). (b) Dependence of the fluorescence emission intensity at 340 nm of SP-B or SP-Br on the concentration of the phospholipid. (c) Scatchard plots of the data from the binding isotherms, where X is P_b/L_T, P_b is the concentration of lipid-bound protein at a given phospholipid concentration (L_T), and P_f is the concentration of free protein. Solid lines are the best fit plots for the binding isotherms.

Table 2: Apparent Parameters for the Interaction of Native SP-B and SP-Br with Phosphatidylcholine Bilayers

	SP-B		SP-Br	
	n	K_D (μM)	n	K_D (μM)[a]
PC	19.2 ± 0.3	9.7 ± 0.1	−	46 5.6
DPPC	20.5 ± 0.3	8.8 ± 0.1	−	15.4 2.3

[a] The curves for binding of SP-Br to phospholipids lead to biphasic Scatchard plots; therefore, two values of K_D have been calculated.

of adsorption under more physiologically relevant conditions, that is, 37 °C, 100% humidity, and high concentrations of SP-B-containing surfactant in the hypophase (*30*). Native SP-B induced rapid increases in surface pressure upon injection of DPPC/SP-B suspensions into the subphase of a surface balance (Figure 7, top panels). DPPC suspensions hardly adsorbed at the interface in the absence of SP-B, under the limiting conditions of our experiments. In the presence of 5 or 10% native SP-B by weight, DPPC produced a similar rapid adsorption up to pressures of 12−15 mN/m, as previously reported (*28*). Interestingly, the presence of SP-Br had even better accelerating effects on the adsorption kinetics of DPPC. Five weight percent SP-Br induced rapid adsorption of DPPC/SP-Br suspensions up to 20 mN/m, and suspensions containing 10% SP-Br reached pressures on the order of 30 mN/m in less than 20 min. SP-Br promoted similarly good interfacial adsorption under the more physiological conditions mimicked by the captive bubble technique

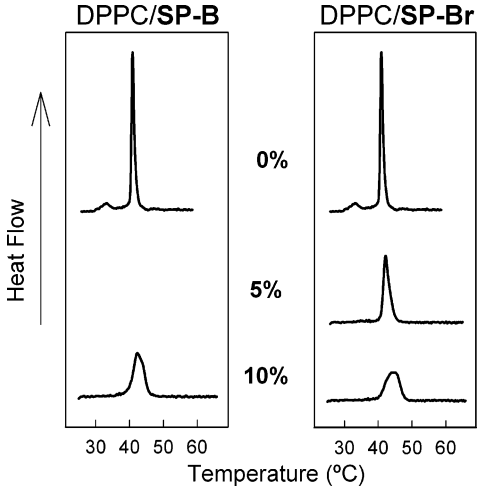

FIGURE 6: Effect of SP-B and SP-Br on the thermotropic properties of DPPC multilamellar suspensions. Differential scanning calorimetry thermograms of DPPC multilamellar suspensions in the absence and presence of the indicated proportions by weight of native SP-B or SP-Br. Scans were obtained on heating at 0.5 °C/min. Five scans were recorded for each sample, from 25 to 70 °C, all of them being qualitatively similar.

(see the bottom panels of Figure 7). Just 1% of either native SP-B or SP-Br promoted rapid adsorption kinetics with either DPPC/PC (70:30, w/w) or DPPC/PG (70:30, w/w) bilayers, to reach surface pressures of 45−50 mN/m close to equilibrium in a few minutes. Bilayers containing SP-Br also followed rapid adsorption kinetics, reaching higher pressures

Table 3: Effect of SP-B and SP-Br on the Parameters of the Thermotropic Phase Transition of DPPC Multilamellar Suspensions, Analyzed by Differential Scanning Calorimetry

	protein/lipid ratio (w/w) (%)	T_m (°C)	ΔH (kcal/mol)
DPPC		41.5	8.3 ± 0.1
DPPC/SP-Br	5	42.1	6.0 ± 0.1
DPPC/SP-Br	10	44.8	5.5 ± 0.3
DPPC/SP-B	10	42.5	5.9 ± 0.1

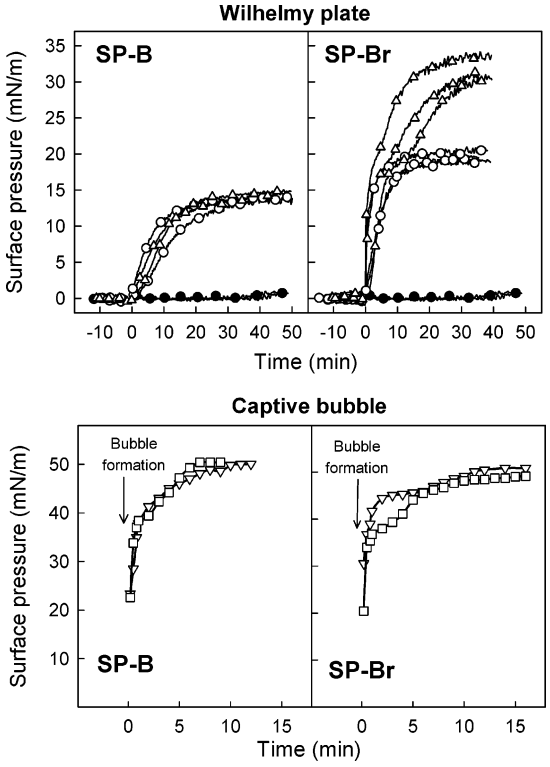

FIGURE 7: Effect of SP-B and SP-Br to promote interfacial phospholipid adsorption. The top panels show interfacial adsorption isotherms of dispersions of DPPC (●) and DPPC with 5% (○) or 10% SP-B (△) (two different experiments shown) or SP-Br (three experiments), by weight, in 5 mM Tris buffer (pH 7) subphases containing 150 mM NaCl and 5 mM $CaCl_2$. Interfacial adsorption was assayed at 25 °C using a specially designed King−Clements surface balance as described in Experimental Procedures. The bottom panels show interfacial adsorption isotherms for dispersions of DPPC/POPC (70:30, w/w) (▽) or DPPC/POPG (70:30, w/w) (□) bilayers, containing 1 wt % SP-B or SP-Br, in 2 mM Tris buffer (pH 7) subphases, containing 150 mM NaCl and 1.5 mM $CaCl_2$. Adsorption was assayed in a custom-designed captive bubble tensiometer (CBT) using a final lipid concentration of 500 μg/mL, at 37 °C, and a representative experiment is shown, after five repetitions.

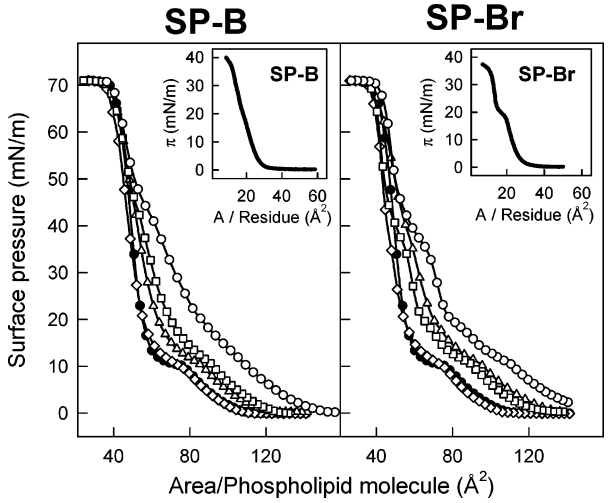

FIGURE 8: Compression isotherms for DPPC/SP-B and DPPC/SP-Br monolayers. Compression $\pi-A$ isotherms for DPPC monolayers (●) and DPPC monolayers containing 2% (◇), 5% (△), 10% (□), or 20% (○) SP-B or SP-Br, by weight, prepared by spreading lipid/protein mixtures in a 3:1 (v/v) $CHCl_3$/MeOH mixture. The subphase in the surface balance was 5 mM Tris buffer (pH 7) containing 150 mM NaCl, and isotherms were obtained at 25 °C and a compression rate of 65 cm^2/min (corresponding to 52.8 $Å^2$ per phospholipid molecule per minute). Insets show $\pi-A$ isotherms of pure proteins, SP-B or SP-Br.

than bilayers containing comparable amounts of native SP-B during the first minutes.

Figure 8 compares the compression isotherms of DPPC films containing different proportions of either native SP-B or SP-Br. Both protein forms introduced similar features into the compression isotherms of DPPC/protein films. The two proteins produced similar progressive expansions of the $\pi-A$ isotherms, indicating that the two protein forms occupy a similar fraction of the interface. The two proteins produced similar broadening of the liquid-expanded/liquid-condensed coexistence plateau of DPPC that was shifted to comparable higher pressures. As previously reported (*28*), isotherms of native SP-B-containing films exhibited a protein squeeze-out plateau at around 48 mN/m, with no indication of lipid exclusion. The isotherms obtained from SP-Br-containing films showed protein squeeze-out plateaus at slightly lower pressures, around 42 mN/m, and an additional plateau at around 20 mN/m. Differences in the isotherms could also be identified in the compression isotherms obtained from pure protein films (insets of Figure 8). The two proteins, native SP-B and SP-Br, produce isotherms with similar lift-off areas of around 30 $Å^2$/residue, indicating that they occupy similar initial molecular areas in the interface at full coverage. Pure native SP-B films collapse at 40 mN/m, while films made of SP-Br collapse at a slightly lower pressure of 38 mN/m, indicating that the reduced form has a slightly lower stability at the interface, as observed also with the protein/lipid films. Finally, the isotherms of pure SP-Br also show a conspicuous transition close to 20 mN/m, reflecting a change in surface disposition that could be also detected, at similar pressures, in the lipid/protein isotherms.

Although native SP-B is squeezed out from phospholipid films when compressed above 48 mN/m, the protein remains associated with the compressed phases and continues to stabilize films against spontaneous relaxation as they are further compressed to high pressures (*28*). This activity of SP-B would be important *in vivo* to aid in maintaining the high pressures required to avoid collapse during the moderately long periods of time needed to empty the lung during expiration. Figure 9 shows that SP-Br retains the ability of SP-B to stabilize compressed DPPC films against spontaneous relaxation. Under the conditions of our experiments, pure DPPC monolayers compressed up to 70 mN/m in a large surface balance, at a relatively rapid speed, undergo a continuous pressure decay once compression is stopped. The presence of 2, 5, and 10 wt % native SP-B markedly decreased the relaxation rate, the maximum effect being observed at 5% SP-B, as previously observed (*28*). The reduced form of the protein, SP-Br, produced a similar

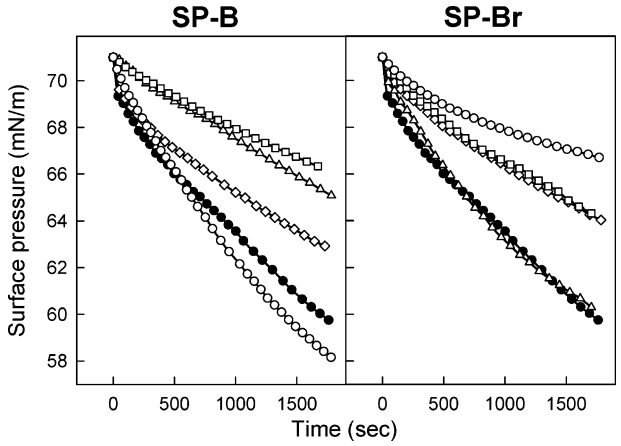

FIGURE 9: Effect of SP-B and SP-Br on the relaxation $\pi-t$ isotherms of compressed DPPC films. Interfacial monolayers were prepared from DPPC solutions in a Chl/MeOH mixture (3:1, v/v) in the absence (●) or presence of 2% (◇), 5% (△), 10% (□), or 20% (○) SP-B or SP-Br, by weight. Plots present the decay of surface pressure vs time of the films once compressed up to 70 mN/m at 65 cm^2/min, and compression is stopped. Experiments were carried out in a 5 mM Tris buffer subphase (pH 7) containing 150 mM NaCl, at 25 °C.

stabilization of compressed DPPC films, which was maintained at the highest protein percents that were tested, 20% protein to lipid by weight. This result strongly suggests that SP-Br adopts a disposition and interaction with the polar face of compressed films similar to that of native SP-B.

The effect of native SP-B and SP-Br in the $\pi-A$ isotherms of lipid/protein films was also examined with the CBT, an instrument that allows comparison of the behavior under more physiologically relevant conditions. Figure 10 shows $\pi-A$ isotherms measured in bubbles formed in suspensions of different native SP-B/lipid or SP-Br/lipid combinations, and subjected to quasi-static compression−expansion cycling. Native SP-B (1 wt %) produced good surface behavior when combined with both zwitterionic [70:30 (w/w) DPPC/POPC] and anionic [70:30 (w/w) DPPC/POPG] lipid mixtures. DPPC/POPC/SP-B films had to be compressed to 40% of the initial surface to produce pressures of around 70 mN/m in the first compression cycle. The subsequent bubble expansion led to an immediate fall in surface pressure, resulting in a marked hysteresis. By the third compression cycle, pressures on the order of 70 mN/m were reached with only 30% compression, and only 20% compression was required for the fifth cycle, leading to a virtual abolition of hysteresis. This film improvement resulted primarily from a reduction in the length of the so-called "squeeze-out" plateau near the equilibrium surface pressure of approximately 47 mN/m. This behavior has been traditionally interpreted as being a consequence of SP-B-induced progressive enrichment of the interfacial film in DPPC, the only phospholipid component able to produce such a high surface pressure with standard balances. In the presence of anionic species, less compression was required initially to produce high surface pressures during the first compression. This arose because of the lack of a squeeze-out plateau but with increased compressibility arising around 60 mN/m. However, with continued cycling, the isotherms progressively approached those obtained with zwitterionic lipids, indicating that after a few cycles, all SP-B-containing films are very similar and resemble almost pure DPPC.

In contrast, the $\pi-A$ isotherms obtained in the presence of SP-Br exhibited very different behavior in the absence or presence of anionic phospholipids. With the zwitterionic system, the squeeze-out plateau was extended so that 60% surface area reduction was required to attain surface pressures near 70 mN/m. In addition, during film expansion, surface pressure continued to fall below 40 mN/m, indicating poor phospholipid respreading. More importantly, with purely zwitterionic lipids, SP-Br did not improve the surface behavior of the lipid/protein films during successive cycling. More than 50% compression was still required for bubbles formed in DPPC/POPC/SP-Br suspensions to reach pressures close to 70 mN/m with the third and fifth compression cycles. This effect was at least partially due to poor respreading and/or adsorption during intercycle delay. As a result, hysteresis remained evident. These results are consistent with both poor respreading with zwitterionic films containing SP-Br and a failure to improve film quality to resemble DPPC-enriched films. In contrast, SP-Br was able to mimic rather well the behavior of native SP-B in the presence of anionic PG. Although a slightly higher compression ratio than that with SP-B was required to attain 70 mN/m during the initial compression, film behavior increasingly improved during successive compression−expansion cycles. This resulted in isotherm profiles closely resembling those with the native protein requiring only 20% surface area reduction during the fifth cycle.

The differences observed when comparing the surface behavior of native SP-B and SP-Br under quasi-static compression−expansion cycling were maintained when the lipid/protein preparations were assayed under the more physiologically relevant dynamic cycling regime (Figure 11). Films containing native SP-B sustained highly reproducible, nonhysteretic, compression−expansion isotherms, independent of the presence or absence of anionic phospholipids. Both DPPC/POPC/SP-B (70:30:1, w/w/w) and DPPC/POPG/SP-B (70:30:1, w/w/w) films could be repeatedly compressed and expanded for more than 20 cycles while maintaining the ability to reach pressures on the order of 70 mN/m with just 15−20% compression. Practically no hysteresis was observed during expansion. Samples containing SP-Br without anionic lipids proved to be very inefficient in reaching high pressures with low compression. After 20 compression−expansion cycles, 60% compression was still required for DPPC/POPC/SP-Br (70:30:1, w/w/w) films to reach 70 mN/m. However, in the presence of POPG, SP-Br-containing films retained excellent isotherm cycling behavior similar to those shown by films containing native SP-B.

DISCUSSION

Several previous studies have suggested the critical importance of cysteines and disulfides for the biophysical activity of SP-B. Some studies, published soon after discovery of SP-B as one of the surface-active proteins in surfactant, pointed out that reduction of the disulfides in SP-B produces a less active protein (*33*). Reduction of disulfides in a protein is usually achieved by simple treatment of the protein with reducing agents such as β-mercaptoethanol or DTT, at varying concentrations. Extensive reduction of disulfides in small proteins with compact folding requires substantial denaturation of the structure (*34*). This is the case, for

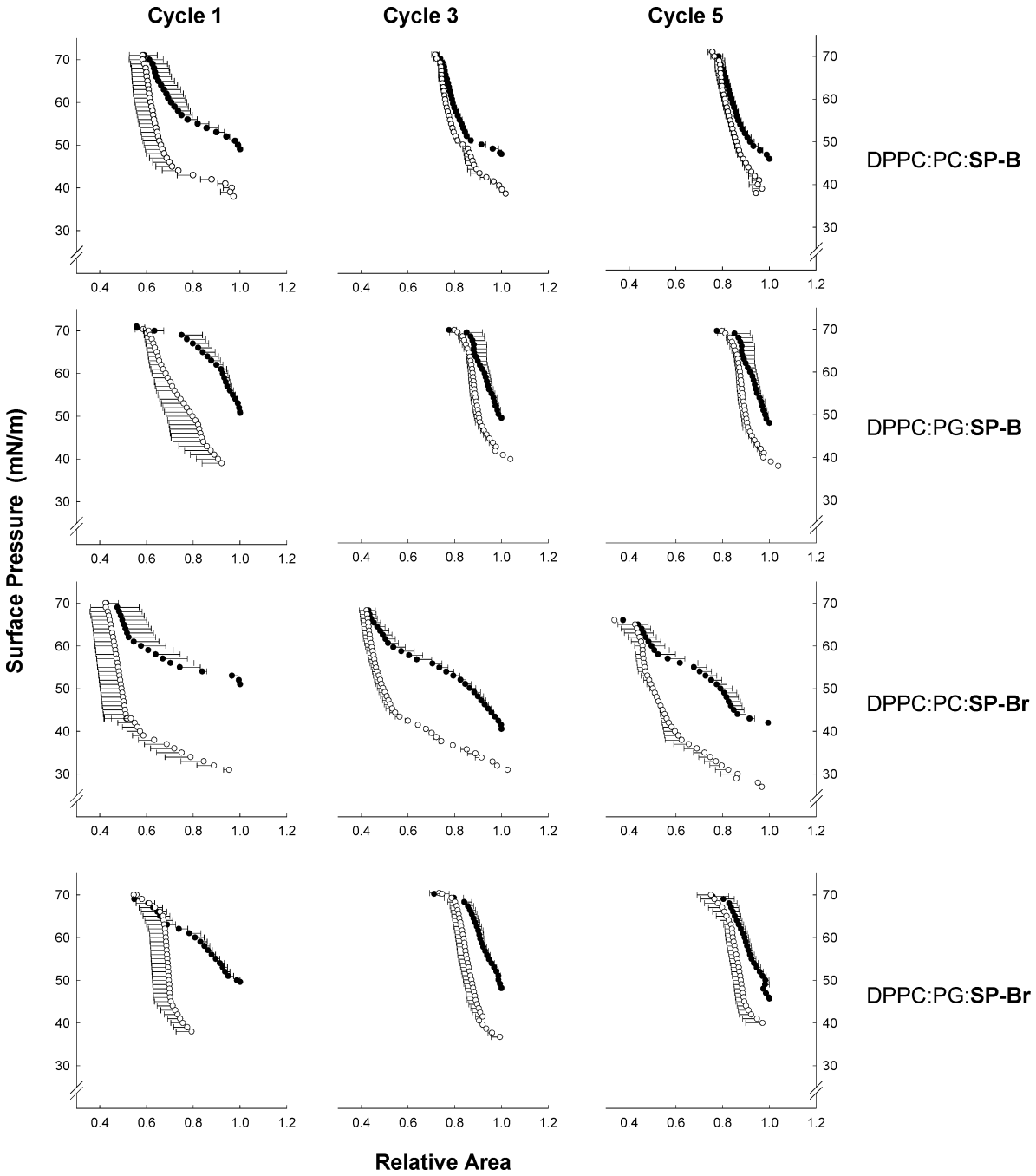

FIGURE 10: Effect of SP-B and SP-Br on the compression−expansion behavior of lipid/protein films under quasi-static conditions. Quasi-static compression (●)−expansion (○) isotherms of DPPC/POPC (70:30, w/w) and DPPC/POPG (70:30, w/w) monolayers in the presence of 1 wt % SP-B or SP-Br. Isotherms were constructed by averaging three independent experiments for the first, third, and fifth compression−expansion cycles. These experiments were performed as described in Experimental Procedures, using a lipid concentration in the CBT chamber of 500 μg/mL, at 37 °C.

instance, for proteins that are substantially homologous with SP-B such as the saposins or sulfate activator protein (*35*, *36*). No reductive treatment as severe as the one used in this work, including extensive denaturation of the protein checked by circular dichroism, has been previously carried out with SP-B. Several recent studies have shown that the structural and biological activities of saposins are maintained after extensive reduction and carboxyamidomethylation of their cysteine residues. Other studies have addressed evaluation of the potential importance of disulfides for the biological activity of SP-B by introducing mutated SP-B genes expressing protein variants lacking specific cysteines in animals with a SP-B knockout genetic background (*37*−*39*). The difficulty in using these *in vivo* models is that frequently the mutated protein phenotype is not compatible with proper folding, stability, and trafficking of the protein in the cellular context. This can produce a null-protein phenotype (*38*) that does not allow a proper evaluation of the role of the cysteines and disulfides in the surface activity itself, once the protein or the lipid−protein complexes are confronted with the air−liquid interface. The biophysical activity of SP-B has been traditionally assessed by evaluation of the ability of the protein to promote rapid adsorption of phospholipids to air−liquid interfaces (*28*, *40*). This activity is not particularly

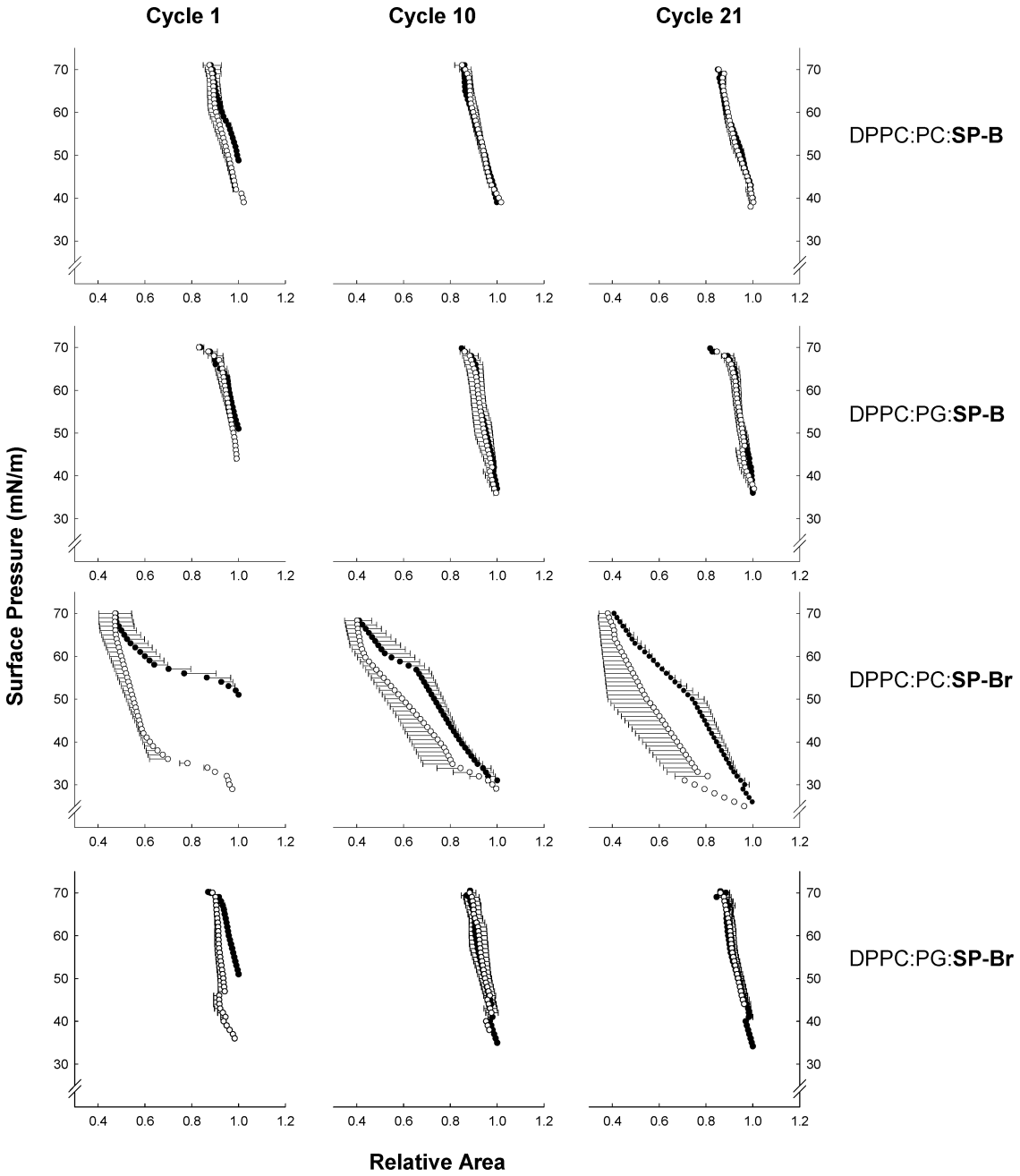

FIGURE 11: Effect of SP-B and SP-Br on the compression−expansion behavior of lipid/protein films under dynamic conditions. Dynamic compression (●)−expansion (○) isotherms of DPPC/POPC (70:30, w/w) and DPPC/POPG (70:30, w/w) bilayers in the presence of 1 wt % SP-B or SP-Br. Isotherms were constructed by averaging three independent experiments for the first, tenth, and 21st dynamic cycles. These experiments were performed as described in Experimental Procedures, using a lipid concentration in the CBT chamber of 500 μg/mL, at 37 °C.

specific, as various proteins and peptides with appropriate levels of hydrophobicity, amphipathicity, and cationicity mimic this SP-B action reasonably well (*41*, *42*). In the presence of SP-B, lipid/protein films require progressively lower levels of relative compression, during successive compression−expansion cycles, to reach the high surface pressures (low surface tensions) thought to be required to stabilize the lung *in vivo* (*43*). This feature has usually been interpreted as SP-B promoting a progressive compression-driven enrichment of the interfacial lipid/protein films in DPPC, the only phospholipid species in surfactant able to produce a surface tension near 0 mN/m (surface pressure of 72 mN/m) under standard compression conditions. Alternatively, SP-B could promote formation during compression of specialized two- or three-dimensional structures permitting the highest pressures. In this study, we have conducted a careful evaluation of the effect of disulfide reduction of SP-B on its structure, lipid−protein interactions, and interfacial dynamics.

We have demonstrated that treatment of SP-B under the conditions optimized in this study produces a highly reduced form, with no remaining intermolecular disulfide bonds. We believe that the protein also lacks most of the intramolecular disulfides, but this has not been proven fully. The fact that this highly reduced protein refolds from a complete denatured state into a structure comparable to that of the native protein is quite remarkable, and indicates that the primary structure of the mature protein probably possesses all of the determi-

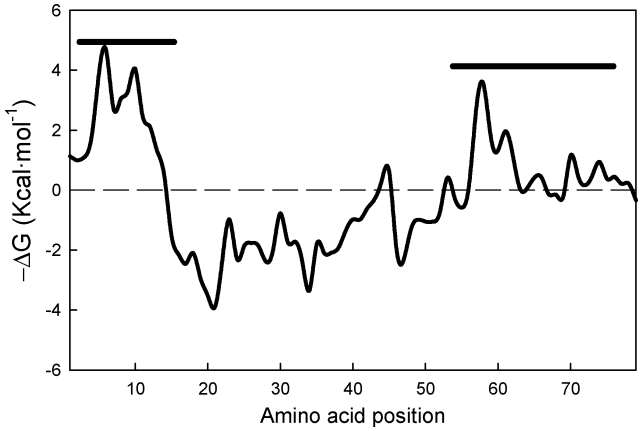

FIGURE 12: Interfacial hydrophobicity profile of the porcine SP-B sequence. The theoretical free energy to partition into a membrane interface has been calculated using the hydrophobicity scale proposed by Wimley and White (*46*) for 11-residue segments of the porcine SP-B sequence and plotted vs sequence position. Two peaks with favorable hydrophobic-at-interface free energies are identified and marked in the sequence.

nants required for acquisition of the native folding. Our results indicate that although the overall folding of SP-Br is comparable to that of native SP-B, opening of disulfides produces a more flexible SP-Br conformation. This would explain the higher susceptibility of the tryptophan in SP-Br to quenching by acrylamide, compared with that of the tryptophan in native SP-B. A higher flexibility in SP-Br would also explain the different behavior of the protein compared with that of native SP-B in regard to the parameters governing interaction of the protein with phospholipid bilayers and its disposition at the air−liquid interface. Native disulfide-cross-linked SP-B behaves as a single membrane-interacting or interface-interacting molecular unit. In contrast, SP-Br exhibits a clearly biphasic behavior when interacting with interfaces, either those offered by lipid membranes or the one in contact with air. Although the three-dimensional structure of SP-B has not been determined, analysis of the sequence and secondary structure of SP-B led to the proposal that the protein possesses several well-defined amphipathic helical segments (*44*, *45*). In the native dimeric protein, these segments are cross-linked to each other by disulfides, probably restricting independent interactions of each segment with biphasic environments. The reduced SP-Br forms could have fewer restrictions, potentially permitting the independent interaction of the helical segments of SP-B with membranes or interfaces. A different affinity of at least two of the segments for phospholipid bilayers could explain the biphasic effect of protein−lipid interactions on the fluorescence properties of SP-Br. One of the regions, presumably the one with less affinity for hydrophobic environments, is squeezed out at around 20 mN/m, while another differentiated region would collapse only at higher pressures, in the order of those producing squeeze-out of the whole native SP-B, around 45 mN/m (Figure 8). Examination of the theoretical interfacial hydrophobicities associated with the SP-B sequence, according to the scale proposed by White and Wimley (*46*) (Figure 12), is consistent with the existence of two distinct hydrophobic interfacial segments in the protein, thereby supporting this interpretation of our experiments. The 15−20 residues at the N-terminal segment of SP-B would define a region with the highest relative affinity for interaction with interfaces, while a region including residues 55−75 of the sequence could also have a tendency to associate with interfaces, although with a potentially less favorable free energy. The affinity of native disulfide-cross-linked SP-B dimers for hydrophobic/hydrophilic interfaces could correlate primarily with that of the N-terminal segment. This feature would explain why synthetic peptides with a sequence corresponding to the 25 N-terminal residues of SP-B mimic many of the lipid−protein interactions and surface activities of full-length SP-B (*47*, *48*). The effect of SP-B on the acyl chain packing of DPPC bilayers could also primarily reflect the effect of the N-terminal segment, which is the one with the highest interfacial hydrophobicity and potentially the one best able to penetrate into deeper regions of the membrane interface. This could be the basis for the similar behavior observed for native SP-B and SP-Br in the calorimetry experiments. Similar modes and extents of interaction of the two protein forms with the phospholipid surface would also allow a similar ability of the two proteins to provide structural support to compressed interfacial films against spontaneous relaxation.

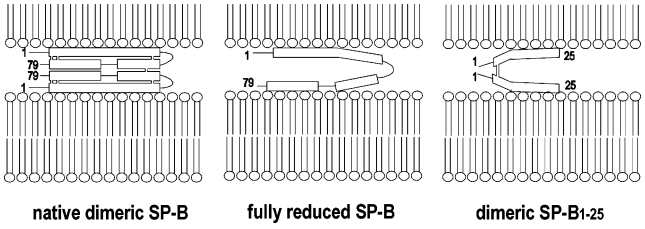

FIGURE 13: Comparative model for the interaction of SP-B, SP-Br, and dimeric SP-B_{1-25} with phospholipid bilayers and monolayers.

Surprisingly, the reduced form of SP-B somehow has a superior ability to promote interfacial adsorption of surfactant phospholipids than the native disulfide cross-linked protein. Such improved activity would most likely arise from the higher conformational flexibility introduced into SP-Br, compared with the native protein. We speculate that the flexibility gained by disulfide reduction in SP-Br probably improves the ability of the protein to promote the association of lipid−protein complexes with the interfacial films. The two distinct membrane-interacting segments in SP-Br could interact with both the interfacial monolayer and an approaching bilayer, thereby facilitating their close apposition and the subsequent movement of lipid molecules between the two structures. The effect of disulfide reduction resembles in this sense the effect observed with dimerization of the synthetic peptide SP-B_{1-25} (*49*). Veldhuizen et al. concluded that dimeric SP-B_{1-25} could better mimic the surface activity of native SP-B because the disulfide connection between the two identical amphipathic segments would allow simultaneous interaction of the dimeric peptide with neighboring lipid structures such as those approaching the surface during surfactant adsorption. As we illustrate in Figure 13, SP-Br may be flexible enough to allow simultaneous interaction with a monolayer and a bilayer, and therefore mimic the active disposition of native SP-B (dimeric) and dimeric SP-B_{1-25}. It has been proposed that native SP-B dimerization, although stabilized by an intermolecular disulfide bond, is primarily promoted by two salt bridges between Arg52 of a monomer and Glu51 of the other monomer and vice versa (*50*). According to this model, SP-Br could also potentially

dimerize by adopting a disposition similar to that of the native protein. Nevertheless, the higher intrinsic flexibility of SP-Br could still better facilitate the initiation of SP-B-promoted bilayer−monolayer contacts contributing to phospholipid adsorption.

Finally, we have observed that SP-Br is also able to reproduce the ability of SP-B to progressively enhance interfacial films during compression−expansion cycling to achieve very low surface tensions (high surface pressures) with minimal compression. Interestingly, PG, the major anionic lipid in pulmonary surfactant, is absolutely required for SP-Br to behave as efficiently as native SP-B. In the absence of PG, SP-Br is not able to improve the surface dynamics of lipid/protein films during compression−expansion cycling, despite the better adsorption activity shown by SP-Br with purely zwitterionic phospholipid−protein complexes. Interactions between SP-Br and PG probably fine-tune the active conformation of the protein which, in the absence of PG, could be either too flexible or altered with respect to the conformation required to refine the films during dynamic cycling. The disulfides in native SP-B could firmly retain an active conformation of the protein that would be capable of refining both zwitterionic and anionic phospholipid/protein films. SP-B secondary structure, including the presence of hydrophobic amphipathic helical segments, could be sufficient for promoting interfacial adsorption. Refining of interfacial films by SP-B during compression is probably more sensitive and requires further organization of the secondary structural elements of the protein in the proper tertiary structure, which is well maintained by disulfides in native SP-B and induced by PG in SP-Br. Such a structure and its functional behavior would in principle be difficult to mimic by simple synthetic peptides. We have previously demonstrated that SP-B binds selectively PG compared with other anionic phospholipids (*51*), and that the interaction of SP-B with PG has significant conformational effects within membrane environments (*52*). We propose that the *in vivo* folding of SP-B to the active conformation, a process that could precede formation of disulfide bonds, could also be assisted by surfactant lipid composition.

We conclude that SP-B-like polypeptides lacking disulfides could still be potentially good mimics of native disulfide-linked SP-B. The amino acid sequence of SP-B apparently contains most of the structural determinants required to define the proper organization of the membrane and surface-active elements of the protein. The appropriate lipid composition of the lipid−protein complexes could, however, be required for generation of the active conformation of SP-B analogues. These findings are relevant for approaches involving production of human SP-B analogues and new SP-B-based therapeutic surfactants.

ACKNOWLEDGMENT

We thank Dr. Jose Luis Lopez-Lacomba from Instituto Pluridisciplinar in Universidad Complutense (Madrid, Spain) for his technical assistance with some of the calorimetry experiments.

REFERENCES

1. Perez-Gil, J., Cruz, A., and Plasencia, I. (2003) Structure−function relationships of hydrophobic proteins SP-B and SP-C in pulmonary surfactant, in *Developments in Lung Surfactant (Dys)Function* (Nag, K., Ed.) Marcel Dekker, New York.
2. Veldhuizen, R., Nag, K., Orgeig, S., and Possmayer, F. (1998) The role of lipids in pulmonary surfactant, *Biochim. Biophys. Acta 1408*, 90−108.
3. Perez-Gil, J. (2001) Lipid−protein interactions of hydrophobic proteins SP-B and SP-C in lung surfactant assembly and dynamics, *Pediatr. Pathol. Mol. Med. 20*, 445−469.
4. Perez-Gil, J., and Keough, K. M. (1998) Interfacial properties of surfactant proteins, *Biochim. Biophys. Acta 1408*, 203−217.
5. Nogee, L. M., Garnier, G., Dietz, H. C., Singer, L., Murphy, A. M., deMello, D. E., and Colten, H. R. (1994) A mutation in the surfactant protein B gene responsible for fatal neonatal respiratory disease in multiple kindreds, *J. Clin. Invest. 93*, 1860−1863.
6. Clark, J. C., Wert, S. E., Bachurski, C. J., Stahlman, M. T., Stripp, B. R., Weaver, T. E., and Whitsett, J. A. (1995) Targeted disruption of the surfactant protein B gene disrupts surfactant homeostasis, causing respiratory failure in newborn mice, *Proc. Natl. Acad. Sci. U.S.A. 92*, 7794−7798.
7. Melton, K. R., Nesslein, L. L., Ikegami, M., Tichelaar, J. W., Clark, J. C., Whitsett, J. A., and Weaver, T. E. (2003) SP-B deficiency causes respiratory failure in adult mice, *Am. J. Physiol. 285*, L543−L549.
8. Merrill, J. D., and Ballard, R. A. (2003) Pulmonary surfactant for neonatal respiratory disorders, *Curr. Opin. Pediatr. 15*, 149−154.
9. Lewis, J. F., and Veldhuizen, R. (2003) The role of exogenous surfactant in the treatment of acute lung injury, *Annu. Rev. Physiol. 65*, 613−642.
10. Whitsett, J. A., and Weaver, T. E. (2002) Hydrophobic surfactant proteins in lung function and disease, *N. Engl. J. Med. 347*, 2141−2148.
11. Johansson, J., Curstedt, T., and Jornvall, H. (1991) Surfactant protein B: Disulfide bridges, structural properties, and kringle similarities, *Biochemistry 30*, 6917−6921.
12. Weaver, T. E. (1998) Synthesis, processing and secretion of surfactant proteins B and C, *Biochim. Biophys. Acta 1408*, 173−179.
13. Gupta, M., Hernandez-Juviel, J. M., Waring, A. J., Bruni, R., and Walther, F. J. (2000) Comparison of functional efficacy of surfactant protein B analogues in lavaged rats, *Eur. Respir. J. 16*, 1129−1133.
14. Johansson, J., Curstedt, T., and Robertson, B. (2001) Artificial surfactants based on analogues of SP-B and SP-C, *Pediatr. Pathol. Mol. Med. 20*, 501−518.
15. Curstedt, T., Jornvall, H., Robertson, B., Bergman, T., and Berggren, P. (1987) Two hydrophobic low-molecular-mass protein fractions of pulmonary surfactant. Characterization and biophysical activity, *Eur. J. Biochem. 168*, 255−262.
16. Perez-Gil, J., Cruz, A., and Casals, C. (1993) Solubility of hydrophobic surfactant proteins in organic solvent/water mixtures. Structural studies on SP-B and SP-C in aqueous organic solvents and lipids, *Biochim. Biophys. Acta 1168*, 261−270.
17. Shevchenko, A., Wilm, M., Vorm, O., and Mann, M. (1996) Mass spectrometric sequencing of proteins silver-stained polyacrylamide gels, *Anal. Chem. 68*, 850−858.
18. Houthaeve, T., Gausepohl, H., Mann, M., and Ashman, K. (1995) Automation of micro-preparation and enzymatic cleavage of gel electrophoretically separated proteins, *FEBS Lett. 376*, 91−94.
19. Wustneck, N., Wustneck, R., Perez-Gil, J., and Pison, U. (2003) Effects of oligomerization and secondary structure on the surface behavior of pulmonary surfactant proteins SP-B and SP-C, *Biophys. J. 84*, 1940−1949.
20. Ruano, M. L., Garcia-Verdugo, I., Miguel, E., Perez-Gil, J., and Casals, C. (2000) Self-aggregation of surfactant protein A, *Biochemistry 39*, 6529−6537.
21. Perczel, A., Park, K., and Fasman, G. D. (1992) Analysis of the circular dichroism spectrum of proteins using the convex constraint algorithm: A practical guide, *Anal. Biochem. 203*, 83−93.
22. Cruz, A., Casals, C., Plasencia, I., Marsh, D., and Perez-Gil, J. (1998) Depth profiles of pulmonary surfactant protein B in phosphatidylcholine bilayers, studied by fluorescence and electron spin resonance spectroscopy, *Biochemistry 37*, 9488−9496.
23. Cruz, A., Casals, C., Keough, K. M., and Perez-Gil, J. (1997) Different modes of interaction of pulmonary surfactant protein SP-B in phosphatidylcholine bilayers, *Biochem. J. 327*, 133−138.
24. Lakowicz, J. R. (1999) *Principles of Fluorescence Spectroscopy*, 2nd ed., Kluwer Academics/Plenum Publishers, New York.

25. Lehrer, S. S. (1971) Solute perturbation of protein fluorescence. The quenching of the tryptophyl fluorescence of model compounds and of lysozyme by iodide ion, *Biochemistry 10*, 3254−3263.
26. Plasencia, I., Cruz, A., Lopez-Lacomba, J. L., Casals, C., and Perez-Gil, J. (2001) Selective labeling of pulmonary surfactant protein SP-C in organic solution, *Anal. Biochem. 296*, 49−56.
27. Camacho, L., Cruz, A., Castro, R., Casals, C., and Pérez-Gil, J. (1996) Effect of pH on the interfacial adsorption activity of pulmonary surfactant, *Colloids Surf. B 5*, 271−277.
28. Cruz, A., Worthman, L. A., Serrano, A. G., Casals, C., Keough, K. M., and Perez-Gil, J. (2000) Microstructure and dynamic surface properties of surfactant protein SP-B/dipalmitoylphosphatidylcholine interfacial films spread from lipid-protein bilayers, *Eur. Biophys. J. 29*, 204−213.
29. Rodriguez-Capote, K., Nag, K., Schurch, S., and Possmayer, F. (2001) Surfactant protein interactions with neutral and acidic phospholipid films, *Am. J. Physiol. 281*, L231−L242.
30. Schurch, S., Bachofen, H., Goerke, J., and Possmayer, F. (1989) A captive bubble method reproduces the in situ behavior of lung surfactant monolayers, *J. Appl. Physiol. 67*, 2389−2396.
31. Plasencia, I., Rivas, L., Keough, K. M., Marsh, D., and Perez-Gil, J. (2003) The N-terminal segment of pulmonary surfactant lipopeptide SP-C has intrinsic propensity to interact with and perturb phospholipid bilayers, *Biochem. J.*
32. Shiffer, K., Hawgood, S., Haagsman, H. P., Benson, B., Clements, J. A., and Goerke, J. (1993) Lung surfactant proteins, SP-B and SP-C, alter the thermodynamic properties of phospholipid membranes: A differential calorimetry study, *Biochemistry 32*, 590−597.
33. Revak, S. D., Merritt, T. A., Hallman, M., Heldt, G., La Polla, R. J., Hoey, K., Houghten, R. A., and Cochrane, C. G. (1991) The use of synthetic peptides in the formation of biophysically and biologically active pulmonary surfactants, *Pediatr. Res. 29*, 460−465.
34. Gasset, M., Mancheno, J. M., Lacadena, J., Martinez del Pozo, A., Onaderra, M., and Gavilanes, J. G. (1995) Spectroscopic characterization of the alkylated α-sarcin cytotoxin: Analysis of the structural requirements for the protein−lipid bilayer hydrophobic interaction, *Biochim. Biophys. Acta 1252*, 43−52.
35. Faull, K. F., Higginson, J., Waring, A. J., To, T., Whitelegge, J. P., Stevens, R. L., Fluharty, C. B., and Fluharty, A. L. (2000) Hydrogen−deuterium exchange signature of porcine cerebroside sulfate activator protein, *J. Mass Spectrom. 35*, 392−401.
36. Faull, K. F., Higginson, J., Waring, A. J., Johnson, J., To, T., Whitelegge, J. P., Stevens, R. L., Fluharty, C. B., and Fluharty, A. L. (2000) Disulfide connectivity in cerebroside sulfate activator is not necessary for biological activity or α-helical content but is necessary for trypsin resistance and strong ligand binding, *Arch. Biochem. Biophys. 376*, 266−274.
37. Zaltash, S., Griffiths, W. J., Beck, D., Duan, C. X., Weaver, T. E., and Johansson, J. (2001) Membrane activity of (Cys48Ser) lung surfactant protein B increases with dimerisation, *Biol. Chem. 382*, 933−939.
38. Beck, D. C., Na, C. L., Whitsett, J. A., and Weaver, T. E. (2000) Ablation of a critical surfactant protein B intramolecular disulfide bond in transgenic mice, *J. Biol. Chem. 275*, 3371−3376.
39. Beck, D. C., Ikegami, M., Na, C. L., Zaltash, S., Johansson, J., Whitsett, J. A., and Weaver, T. E. (2000) The role of homodimers in surfactant protein B function in vivo, *J. Biol. Chem. 275*, 3365−3370.
40. Wang, Z., Gurel, O., Baatz, J. E., and Notter, R. H. (1996) Differential activity and lack of synergy of lung surfactant proteins SP-B and SP-C in interactions with phospholipids, *J. Lipid Res. 37*, 1749−1760.
41. Cochrane, C. G., and Revak, S. D. (1991) Pulmonary surfactant protein B (SP-B): Structure−function relationships, *Science 254*, 566−568.
42. McLean, L. R., and Lewis, J. E. (1995) Biomimetic pulmonary surfactants, *Life Sci. 56*, 363−378.
43. Nag, K., Munro, J. G., Inchley, K., Schurch, S., Petersen, N. O., and Possmayer, F. (1999) SP-B refining of pulmonary surfactant phospholipid films, *Am. J. Physiol. 277*, L1179−L1189.
44. Cruz, A., Casals, C., and Perez-Gil, J. (1995) Conformational flexibility of pulmonary surfactant proteins SP-B and SP-C, studied in aqueous organic solvents, *Biochim. Biophys. Acta 1255*, 68−76.
45. Vincent, J. S., Revak, S. D., Cochrane, C. G., and Levin, I. W. (1991) Raman spectroscopic studies of model human pulmonary surfactant systems: Phospholipid interactions with peptide paradigms for the surfactant protein SP-B, *Biochemistry 30*, 8395−8401.
46. Wimley, W. C., and White, S. H. (1996) Experimentally determined hydrophobicity scale for proteins at membrane interfaces, *Nat. Struct. Biol. 3*, 842−848.
47. Lipp, M. M., Lee, K. Y., Zasadzinski, J. A., and Waring, A. J. (1996) Phase and morphology changes in lipid monolayers induced by SP-B protein and its amino-terminal peptide, *Science 273*, 1196−1199.
48. Gordon, L. M., Lee, K. Y., Lipp, M. M., Zasadzinski, J. A., Walther, F. J., Sherman, M. A., and Waring, A. J. (2000) Conformational mapping of the N-terminal segment of surfactant protein B in lipid using ^{13}C-enhanced Fourier transform infrared spectroscopy, *J. Pept. Res. 55*, 330−347.
49. Veldhuizen, E. J., Waring, A. J., Walther, F. J., Batenburg, J. J., van Golde, L. M., and Haagsman, H. P. (2000) Dimeric N-terminal segment of human surfactant protein B (dSP-B(1−25)) has enhanced surface properties compared to monomeric SP-B(1−25), *Biophys. J. 79*, 377−384.
50. Zaltash, S., Palmblad, M., Curstedt, T., Johansson, J., and Persson, B. (2000) Pulmonary surfactant protein B: A structural model and a functional analogue, *Biochim. Biophys. Acta 1466*, 179−186.
51. Perez-Gil, J., Casals, C., and Marsh, D. (1995) Interactions of hydrophobic lung surfactant proteins SP-B and SP-C with dipalmitoylphosphatidylcholine and dipalmitoylphosphatidylglycerol bilayers studied by electron spin resonance spectroscopy, *Biochemistry 34*, 3964−3971.
52. Cruz, A., Marsh, D., and Perez-Gil, J. (1998) Rotational dynamics of spin-labelled surfactant-associated proteins SP-B and SP-C in dipalmitoylphosphatidylcholine and dipalmitoylphosphatidylglycerol bilayers, *Biochim. Biophys. Acta 1415*, 125−134.

BI048781U